APPLICATION OF HYPERION DATA TO AGRICULTURAL LAND CLASSIFICATION AND VEGETATION PROPERTIES ESTIMATION IN SWITZERLAND

S. Eckert, M. Kneubühler

[a] Remote Sensing Laboratories (RSL), University of Zürich, Winterthurerstrasse 190, 8057 Zürich, Switzerland - (seckert, kneub)@geo.unizh.ch

WG VII/1 – Fundamental Physics and Modelling (TS)

KEY WORDS: Agriculture, Land Cover, Classification, Remote Sensing, Hyper Spectral, Object, Vegetation, Contextual

ABSTRACT:
On August 18, 2002, the Hyperion hyperspectral imager onboard the EO-1 platform recorded data over an intensively used agricultural area in north western Switzerland, the Limpach Valley. The sensor's 198 spectral bands between 400 and 2500 nm (Level 1B1) and a spatial resolution of 30 m bear the potential for both a detailed land use classification and an accurate estimation of biophysical and biochemical properties of heterogeneously vegetated areas. This study evaluates the potential of HYPERION data for land use classification and vegetation properties estimation (e.g., LAI) in a typical Swiss agricultural environment with its small-spaced fields. A Spectral Angle Mapper approach and a multi-scale object-oriented method are applied for agricultural land use determination. The results show, that the phenological stages of the cultivars are the main factors influencing the separability of agricultural classes and therefore determining the accuracies of the methods applied.

1. INTRODUCTION

1.1 Overview

The growing need for quantitative studies on biogeophysical and –chemical processes in vegetation analysis for agricultural purposes on the one hand, and ecosystem functioning on the other hand, imply both higher spectral and spatial resolution of spaceborne remote sensing devices, together with improved radiometric performance and accurate geolocation. The HYPERION sensor onboard NASA's Earth Observing 1 (EO-1) satellite is the first spaceborne hyperspectral instrument to acquire both visible/near-infrared (400-1000 nm) and shortwave infrared (900-2500 nm) spectral data. With its 242 potential bands and a spatial resolution of 30 m, the sensor bears the potential to provide data for both a detailed land use classification and an accurate estimation of biogeophysical and –chemical properties of heterogeneously vegetated areas.
In this study, the suitability of HYPERION data for land use classification and vegetation properties estimation in a typical Swiss agricultural environment with its small-spaced fields is evaluated. Land use determination from spectral data is performed using both a well established hyperspectral approach (Spectral Angle Mapper) and a multi-scale object-oriented method which allows to derive meaningful image segments on the one hand and to describe the segment's physical and contextual characteristics on the other hand. The potential of the hyperspectral dataset for vegetation properties estimation (e.g., LAI) within single cultivars is approached by assessing the spectral variability of dedicated fields.

1.2 Study Site Location

The Limpach Valley, being the study site of this work, is an intensively cultivated agricultural area in northwestern Switzerland with more than 2000 individual fields. The climate of the Limpach Valley can be regarded as typical for the Swiss Midlands. Precipitation is even to moderatly dry. The vegetation period lasts between 210-230 days. The summer months are characterized by hot temperatures and occasional dry periods [Kneubühler, 2002]. The main agricultural cultivars in the area are maize, potatoes, wheat, barley, canola and sugar beet. Besides, both intensively and extensively used types of grassland can be found. In August, after harvest of the majority of the cereals, the visual impression of the valley is dominated by stubble-fields and bare soil. A detailed ground-truth dataset consisting of more than 50 fields was recorded in the field in order to verify the results of the two land use determination approaches performed in this study. However, in the ground-truth data some crops are represented by only two or three fields.

1.3 HYPERION Hyperspectral Data

HYPERION data were acquired over the Limpach Valley test site on August 18, 2002 at 09:05:42 UTC. The EO-1 satellite is in a sun-synchronous orbit at 705 km altitude. HYPERION images 256 pixels with a nominal size of 30 m on the ground over a 7.65 km swath. Well-calibrated data (Level 1B1) is routinely available. Post-Level 1B1 processing of the dataset, as performed in this study, includes correction for striping pixels, atmospheric correction and georectification.
HYPERION data is acquired in pushbroom mode with two spectrometers. One operates in the VNIR range (70 bands between 356-1058 nm with an average FWHM of 10.90 nm) and the other in the SWIR range (172 bands between 852-2577 nm, with an average FWHM of 10.14 nm). Of the 242 Level 1B1 bands, 44 are set to zero by software during Level 1B1 processing (bands 1-7, 58-76, 225-242).

2. REMOTE SENSING DATA PREPARATION

Post-Level 1B1 data processing of the acquired HYPERION scene contains correction for striping pixels, a scene-based atmospheric correction using ATCOR-4 [Richter] and a georectification procedure, as described in this section.

2.1 Striping Pixels Correction

Especially the first 12 VNIR bands and many SWIR bands of HYPERION are influenced by striping. Stripes are caused by calibration differences in the detector array, since the HYPERION sensor acquires data in pushbroom mode with a separate detector for each column and each band [Goodenough et al., 2003]. Whereas several types of abnormal pixels are corrected during Level 1B1 processing, the case of intermittent striping pixels with lower DN values compared to their neighboring pixels still exists. A correction algorithm [Goodenough et al., 2003] to detect and correct these pixels is applied to this study's dataset. The algorithm traverses each band horizontally to compare each pixel's DN value with the value of its immediate left and right neighboring pixels. A pixel is labeled as a potential abnormal pixel if its DN value is smaller than the DN's of both neighbors. Afterwards, each band is traversed vertically to count the number of consecutive potential abnormal pixels in each column. Given the number of consecutive potential abnormal pixels exceeds a user defined threshold value and the percentage of abnormal pixels in a column is also greater than a user defined threshold value, then the column consists of abnormal pixels and it is marked as a stripe. Finally, the abnormal pixels' DN values are replaced with the average DN values of the immediate left and right neighboring pixels, assuming that nearby pixels have the highest spatial autocorrelation with a center pixel [Goodenough et al., 2003]. The abnormal pixel detection algorithm performed well for most bands, except for intensively striped ones.
Consecutively, an MNF transformation is applied to the dataset in order to further segregate spatially structured striping noise from the actual image data. A total of 15 transformed MNF-bands containing the coherent images are retained in the data for the inverse MNF transformation. In the end, 167 bands out of a total of 242 are chosen for further processing and data analysis. Excluded bands comprise those set to zero, bands in the overlap between the two spectrometers, and bands affected by atmospheric water vapour and heavy noise, which can easily be identified by visual inspection of the image data [Datt et al., 2003].

2.2 Atmospheric Correction

Atmospheric correction of the generated 167 channel HYPERION dataset is performed using ATCOR-4 [Richter, 2003], an atmospheric correction program based on look-up tables generated with a radiative transfer code (MODTRAN-4). An inflight calibration approach based on two targets in the scene is chosen with in-situ measured spectroradiometric ground-truth data (ASD FieldSpec Pro FR Spectroradiometer). The composition of the atmosphere is characterized assuming a typical Limpach Valley summer scenario in terms of water vapour content, aerosol type and optical thickness during HYPERION data take on August 18, 2002.

2.3 Geometric Correction

For orthorectification of the HYPERION scene, the software package PCI Geomatica OrthoEngine is chosen, which uses the parametric sensor model [Toutin, 1985]. The dataset with its 167 bands has to be divided into 5 smaller datasets due to software restrictions, consisting of about 22 bands, which are imported with the corresponding orbit and scene parameters. 26 ground control points (GCPs) and 9 independent check points (ICPs) are collected from a previously orthorectified SPOT 4 scene and transferred to all datasets. The root mean square (RMS) residuals of the GCPs from the CCRS parametric model are 6.4 m in X and 8.4 m in Y directions, respectively. The RMS errors of the ICPs are 8.3 m and 15.4 m in X and Y directions, respectively. For orthorectification the 25-m pixel spacing digital terrain model (DTM) of Switzerland, DHM25, is applied. The nearest neighbor resampling method is used to preserve the blocky structure of the agricultural fields and the original radiometry of the image.

3. METHODOLOGY

Land use classification from HYPERION data in the Limpach Valley is performed based on both a pixel-oriented classification approach (Spectral Angle Mapper, SAM) and a multiscale object-oriented method, which bears the potential to classify pixels not only based on their spectral information, but also by their texture and local context. The results of the two methods are discussed and compared and an accuracy assessment is performed. The accuracies are determined through a pixel to pixel comparison and expressed as *overall*, *producer*, *user* and *inclass accuracy* [Story & Congalton, 1986].

3.1 Spectral Angle Mapper (SAM)

The Spectral Angle Mapper [Boardman & Kruse, 1994] is a technique to classify hyperspectral data by determining the similarity between an endmember spectrum (considered as an n-dimensional vector, where n is the number of bands) and a pixel spectrum in an n-dimensional space. Smaller angles represent closer matches to the reference spectrum. Since this method uses only the direction of a vector and not its length, it is insensitive to illumination and albedo effects. Image-based endmember spectra of the main agricultural land use types in the test area are used as input for Spectral Angle Mapper classification.

3.2 Multiscale Object-Oriented Approach

eCognition[1] software is the first commercially available product for object-oriented and multi-scale image analysis. As opposed to most other pattern recognition algorithms which operate on a pixel-by-pixel basis, eCognition segments a multispectral image into homogeneous objects, or regions, based on neighboring pixels and spectral and spatial properties. The segmentation algorithm does not only rely on the single pixel value, but also on pixel spatial continuity (texture, topology). The resulting formatted objects have not only the value and statistic information of the pixels that they consist of but also carry texture, form (spatial features) and topology information in a common attribute table. The user interacts with the procedure and, based on statistics, texture, form and mutual relations among objects, defines training areas. Image segmentation can be performed at different levels of resolution, or granularity as seen in Figure 1. It is controlled by a user-defined threshold called scale parameter. A higher scale parameter will allow more merging and consequently bigger objects, and vice versa. The homogeneity criterion is a combination of color respectively spectral values and shape properties (shape splits up in smoothness and compactness). By applying different scale parameters and color/shape combinations, the user is able to create a hierarchical network of image objects. For the classification of the segments, two types of nearest neighbor expressions can be used in eCognition: the nearest neighbor (NN) and the standard nearest neighbor (Std. NN) expression. The NN expression and its feature space can be individually

[1] Definiens AG, Trappentreustr. 1, 80339 Munich, Germany

adjusted to classes, membership functions introduced and fuzzy rule applied, whereas the Std. NN expression works with a defined feature space for selected classes. Classification can be performed at different levels of the classification hierarchy. Multi-level segmentation, context classification and hierarchy rules are also available [Baaz et al., 2003].

The first two levels of image objects are segmented representing different scales. The scaling parameter used for level 3 is 65, which should create segments of forested, urban and agricultural areas. The homogeneity criterion parameters are set as follows: color: 0.8, shape: 0.2, smoothness: 0.4 and compactness: 0.6. The HYPERION bands 11, 19, 32, 110, 140 and 190 are given a weighting factor of 5, whereas the remaining channels are given a factor of 1. The HYPERION bands are selected visually based on high spectral contrasts between forested and urban areas and in between agricultural fields.

In a next step, level 1 is created, which should deliminate agricultural fields. A scaling parameter of 27 is chosen and the following homogeneity criterion parameters set: color: 0.9, shape 0.1, smoothness: 0.4, compactness: 0.6. The HYPERION bands 11 and 110 are given a weighting factor of 4, the bands 19, 31, 140 and 190 are given a weighting factor of 2, the remaining channels are not considered in the segmentation process. The extracted image objects on both levels contain the information needed for classifying agricultural fields separated from all surrounding land covers, e.g., forest and urban areas. However, individual but spectrally homogeneous fields are sometimes merged or fields are separated into several smaller segments due to spectral in-field variation.

On level 3 the classes forest, urban areas and agriculture are classified by selecting representative samples of the classes forest, urban areas and agriculture, and applying the Std. NN classifier. Merging segmentation classes forest and urban areas from level 3 with agricultural field segments of level 1 by applying classification-based segmentation results in level 2. This level consists of optimal segments for agricultural field classification.

The class hierarchy is the frame to create the knowledge base for a given classification task. It contains all classes and is organized in a hierarchical structure. Class descriptions are beeing passed down from parent classes to their child classes. Child classes can inherit descriptions from more than one parent class. The purpose of a hierarchical structure is to reduce redundancy and complexity in the class descriptions [Baaz et al., 2003]. The developed class hierarchy for this land use classification is illustrated in Figure 2.


Segmentation level 3

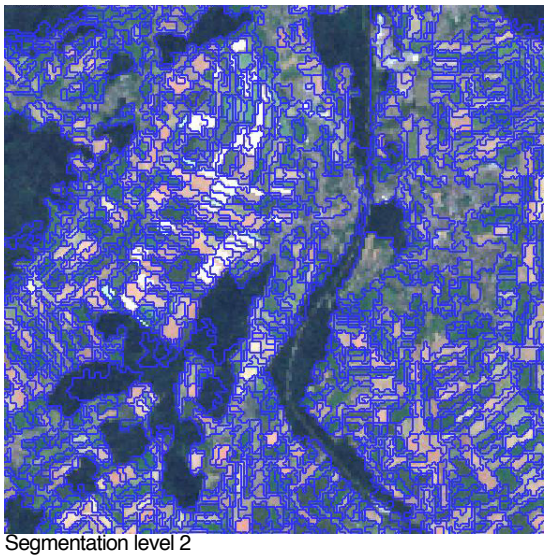
Segmentation level 2

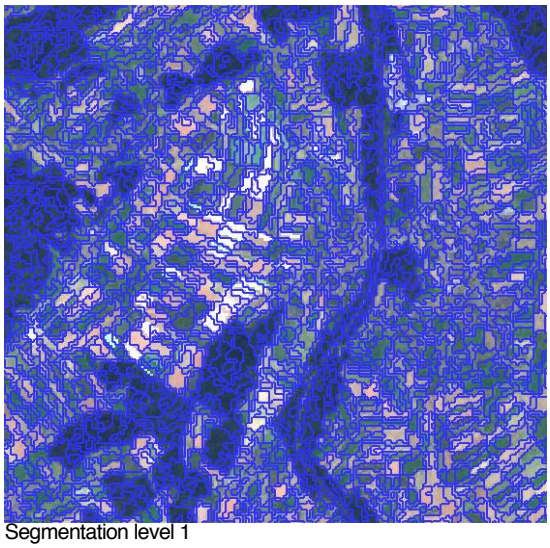
Segmentation level 1

Figure 1. Different levels of segmentation.

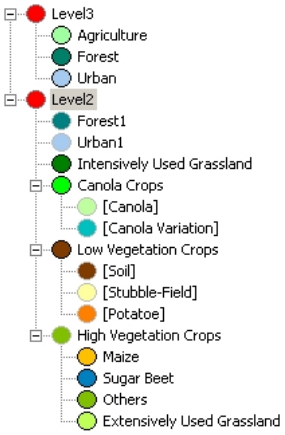

Figure 2. Class hierarchy showing the different levels of classification and classes respectively. Classes in brackets can not be reasonably seperated from each other.

3.3 Spectral In-field Variability Assessment

The retrieval of biogeophysical and –chemical parameters from hyperspectral data implies detectable gradients present in the spectral data. Such variations bear the potential for in-field parameter estimation from hyperspectral data.
In this study, the potential of assessing in-field variations of green LAI (leaf area index) from HYPERION data in a small-spaced heterogeneously vegetated area is investigated, in addition to the classification efforts described in Section 3.1. and Section 3.2. Spectral in-field variation of a single field is quantified as percent deviation of ± 1 standard deviation from mean field reflectance. LAI is an important biogeophysical parameter retrievable from remote sensing data and serves as input into numerous ecosystem models and crop growth models. LAI retrieval in this study is based on a semi-empirical approach proposed by [Clevers et al., 1994]. A corrected near-infrared reflectance, known as Weighted Difference Vegetation Index (WDVI), is calculated by subtracting the contribution of the soil from the measured reflectance. The WDVI is then used for estimation of LAI according to the inverse of an exponential function, as given in Equation 1:

$$LAI = -\frac{1}{\alpha} * \ln\left(1 - \frac{WDVI}{\rho_{\infty}(\lambda_{NIR})}\right) \qquad (1)$$

where LAI = Leaf Area Index, $WDVI$ = Weighted Difference Vegetation Index, α= complex combination of extinction and scattering coefficients, and $\rho_{\infty}(\lambda_{NIR})$ = asymptotically limiting value of the WDVI at very high LAI values.

Standard values for α and $\rho_{\infty}(\lambda_{NIR})$ are taken from literature [Bouman et al., 1992, Clevers et al., 1994].

4. RESULTS

4.1 Land Use Classification Results

Figure 3 indicates that due to the late date of HYPERION data acquisition from a phenological point of view (August 18), either well established fields (maize, sugar beet, grassland) on the one hand or strongly senescing cultivars (canola, potatoes) and harvested (cereal stubble-fields) or bare soil plots on the other hand can be found in the test area. Under such conditions, the discrimination of different land use types with comparable spectral signatures is a challenging task.
Table 1 presents the class specific accuracies achieved with the Spectral Angle Mapper approach. It can be seen that the classes maize, intensively used grassland and stubble-fields can be classified best.

Land Use Type	User Accuracy	Producer Accuarcy	Inclass Accuracy
Maize	0.7919	0.5198	0.8429
Intensively used grassland	0.5764	0.4854	0.5570
Potatoe	0.2747	0.2315	0.1678
Canola	0.2143	0.1818	0.1224
Stubble-fields	0.7062	0.5170	0.7405
Extensively used grassland	0.1045	0.2692	0.0886
Sugar beet	0.0562	0.3571	0.0538
Soil	0.1758	0.4103	0.1633
Canola variation	0.0526	0.3333	0.0500
Overall Accuracy	**0.4396**		
Kappa Accuracy	**0.3377**		

Table 1. Spectral Angle Mapper accuracies determined on a pixel-by-pixel basis for the main land use types present in the Limpach Valley test area.

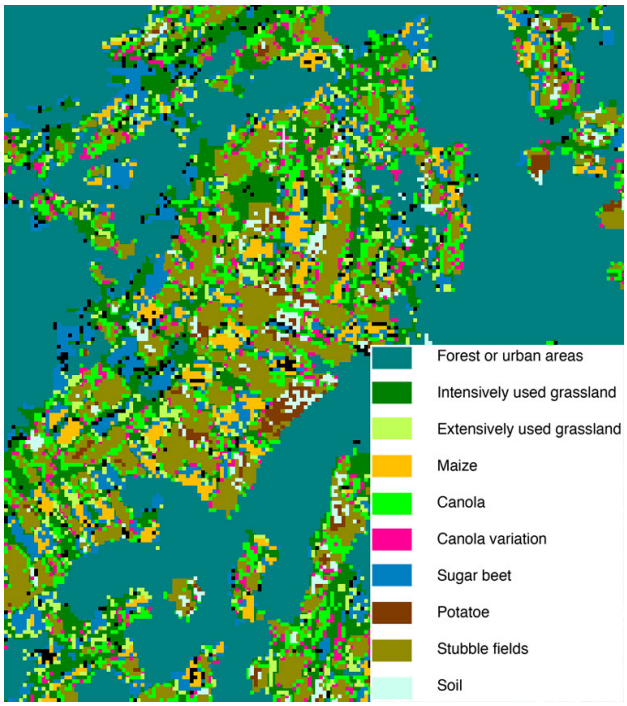

Figure 3. Land use classification result based on a Spectral Angle Mapper (SAM) approach.

Due to the spectral similarity of several classes (see Figure 5), potatoes are manly classified as stubble-fields, canola mainly as stubble-fields or potatoes, and extensively used grassland as maize or intensively used grassland. Sugar beet is often found as maize or grassland, bare soil as stubble-fields or potatoes and the discrimination between the two canola variations was not successful, either.

The object-oriented classification approach has the advantage to prevent from the "salt-and-pepper"-effect as it can be observed in pixel-based classification approaches (e.g., SAM, Figure 3). Nevertheless, if the developed class hierarchy is instable, whole segments (groups of pixels) and not only a pixel are misclassified which results in a low accuracy compared to the ground-truth data. This fact has to be taken into account while interpreting the results.
Classes such as intensively used grassland, maize, sugar beet and canola crops can easily be classified by using samples and manually defined membership functions. Classes with similar spectral characteristics, as illustrated in Figure 5, can not be reasonably separated. Therefore, the classes potatoes, stubble-fields and soil are consolidated into a parent class, as well as the classes canola and canola variation. Table 2 shows the accuracies for the object-oriented classification method.
Intensively used grassland is often misclassified as sugar beet and vice versa. The same misclassification ocurred between canola crops and low vegetation crops. Their spectral reflectances are similar, as can be seen in Figure 5. Since there are only 12 pixels of extensively used meadows available in the ground-truth data, and all misclassified, accuracy is zero. They are either classified as maize or intensively used grassland.

Land Use Type	User Accuracy	Producer Accuarcy	Inclass Accuracy
Maize	0.9068	0.6114	1.3544
Intensively used grassland	0.3978	0.6167	0.4684
Low vegetation crops	0.8712	0.5413	1.0050
Canola crops	0.0421	0.1026	0.0317
Sugar beet	0.0869	0.6667	0.0899
Extensively used grassland	0.0000	0.0000	0.0000
Overall Accuracy	**0.5402**		
Kappa Accuracy	**0.3857**		

Table 2. eCognition classification accuracies determined on a pixel-by-pixel basis for the distinguishable land use classes.

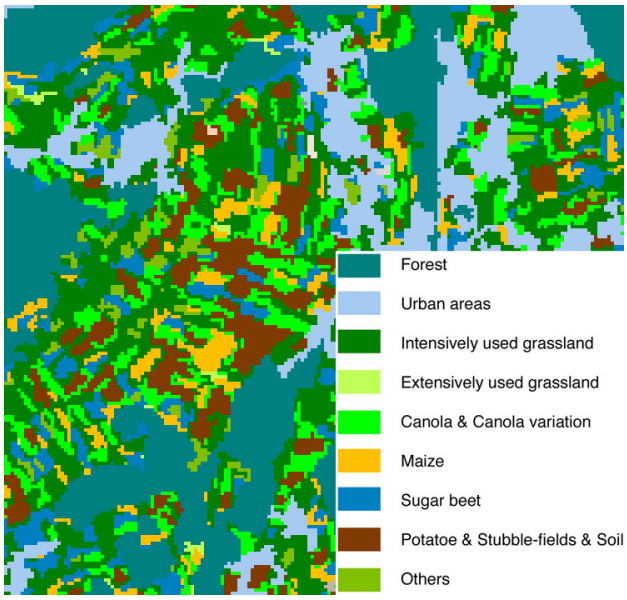

Figure 4. Land use classification result based on object-oriented classification method with eCognition.

4.2 In-field Variation and LAI Estimation Results

In Figure 5, mean reflectance data from HYPERION and the ±1 standard deviation of the data from the mean for representative fields of the various land use types present in the area under investigation are given. The spectral in-field variation, as a wavelength dependent percentage of ±1 standard deviation of the data from the mean, is shown in Figure 6.

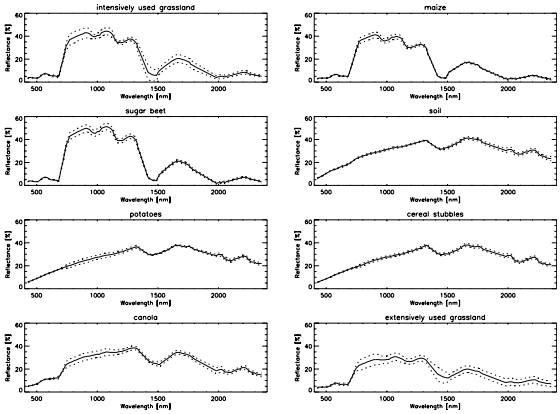

Figure 5. HYPERION spectral data of the main land use types present in the Limpach Valley test area. The mean reflectances of representative fields are given as solid line, the reflectance of ± 1 standard deviation of the data from mean is shown as dotted lines.

Green LAI variations within two selected fields of sugar beet and late stage potatoes are determined based on the WDVI. The fields' infra-red reflectances at 760 nm and red reflectances at 670 nm are used, together with literature values of α and $\rho_{\infty}(\lambda_{NIR})$ for sugar beet and senescing potatoes.
The spectral variation of the two cultivars does not exceed 10% in the VIS/NIR region of the spectrum (see Figure 6). The resulting LAI variations are given in Table 3.

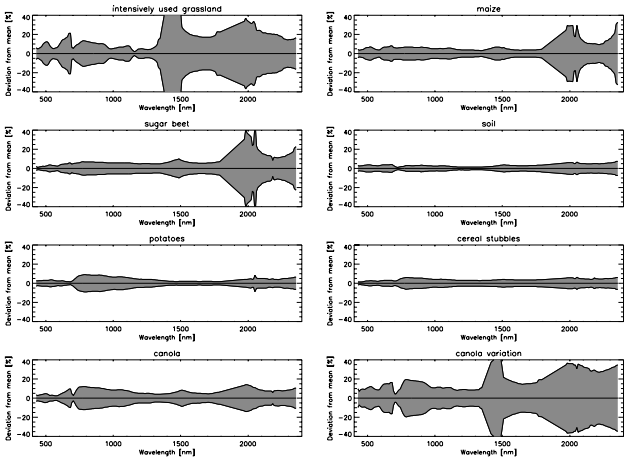

Figure 6. HYPERION spectral in-field variation of the main land use types present in the Limpach Valley test area, represented as percent deviation of ± 1 standard deviation from mean reflectance.

Land Use Type	LAI min	LAI mean	LAI max
Sugar beet	2.92	3.36	3.90
Senescing potatoes	0.03	0.09	0.15

Table 3. In-field variation of green LAI determined from HYPERION data for sugar beet and senescing potatoes. The variation of LAI is calculated based on the spectral variation of the WDVI.

It can be concluded, that in-field variations of green LAI can be retrieved from HYPERION spectral data, with mean values of LAI representing the lush green status of sugar beet and the almost completely senesced phenological stage of the potatoes cultivars.

5. CONCLUSIONS

Two approaches were applied in this work for hyperspectral image classification from HYPERION data: SAM and an object-oriented analysis. Both methods greatly suffer from low spectral variations among the different agricultural land cover types due to the late phenological stage of the cultivars at the time of data take.

With the exception of the classes maize, stubble-fields and intensively used grassland, the majority of agricultural fields could not be classified successfully by applying a Spectral Angle Mapper algorithm. As a consequence of the late phenological stages, the spectral behaviour of various land cover types is very similar. In addition, the small-spaced pattern of many fields in the area produces numerous mixed pixels at HYPERIONS's ground resolution of 30 m, which further decreases the classification accuracy. However, the spectral in-field variation of single fields observable by HYPERION bears the potential of retrieving biogeophysical and –chemical variations within fields, as could be demonstrated in the case of LAI.

Classification results for the object-oriented classification method are disapointing due to several reasons: (a) low spectral variation at dataset-specific acquisition time; most crops are either already harvested or senesced, (b) classification rules for agricultural crop classes for this study are mainly based on spectral features and do not imply relational, textural or shape features, (c) crop fields in Switzerland are small in size and textural differences in HYPERION datasets are low due to the sensor's geometric resolution and (d) relations between crop types are inexistent and cultivation changes every season. eCognition's advances of implying relational, textural or shape features in its hierarchical classification process can unfortunately not be applied to this land use classification.

Agricultural land use classification from HYPERION data is expected to yield better results if the dataset was acquired at the most promising time of year from a spectral point of view, i.e., during the growing season of most agricultural crops in June. Vitality-related crop type specific charcteristics have their largest impact on spectral behaviour at this time of year. As can be seen from the results in Figure 3 and Figure 4, the small-spaced structure of Swiss agricultural fields can partionally be met by HYPERION's ground resolution, although mixed pixels remain a common problem. However, the potential of an object-oriented approach based on relational, textural and shape features can not be fully exploited in agricultural applications due to HYPERION's coarse spatial resolution for such techniques.

6. REFERENCES

Baaz, M. et al., 2003. eCognition User Guide V. 3.0. http://www.definiens-imaging.com/ (accessed 24 Apr. 2003).

Boardman, J.W., and Kruse, F.A., 1994. Automated Spectral Analysis: A Geological Example Using AVIRIS Data, North Grapevine Mountains, Nevada. *Proc 10th Thematic Conference on Geological Remote Sensing*, Environmental Research Institute of Michigan, San Antonio (TX), pp.407-418.

Bouman, B.A.M., van Kasteren, H.W.J., and Uenk, D., 1992. Standard Relations to Estimate Ground Cover and LAI of Agricultural Crops from Reflectance Measurements. *Europ. J. Agronomy*, 4, pp.249-262.

Clevers, J.G.P.W., Büker, C., van Leeuwen, H.J.C., and Bouman, B.A.M., 1994. A Framework for Monitoring Crop Growth by Combining Directional and Spectral Remote Sensing Information. *Remote Sens. Environ.*, 50, pp.161-170.

Datt, B., McVicar, T.R., Van Niel, T.G., Jupp, D.L.B., and Pearlman, J.S, 2003. Preprocessing EO-1 Hyperion Hyperspectral Data to Support the Application of Agricultural Indexes. *IEEE Trans. Geosci. Remote Sensing*, 41(2), pp.1246-1259.

Goodenough, D.G., Dyk, A., Niemann, O., Pearlman, J.S., Chen, H., Han, T., Murdoch, M., and West, C., 2003. Processing HYPERION and ALI for Forest Classification. *IEEE Trans. Geosci. Remote Sensing*, 41(2), pp.1321-1331.

Kneubühler, M., 2002. Spectral Assessment of Crop Phenology Based on Spring Wheat and Winter Barley. *Remote Sensing Series* 38, University of Zürich, Switzerland, pp.149.

Richter, R., 2003. Atmospheric / Topographic Correction for Airborne Imagery. ATCOR-4 User Guide, Version 3.0, DLR-IB 564-02/03, *DLR*, Wessling, Germany, pp.66.

Story, M., and Congalton, R., 1986. Accuracy Assessment: A User's Perspective. *PE&RS*, 52(3), pp.397-399.

Toutin, T., 1985. Analyse mathématique des possibilités cartographiques du système de Spot. Ph.D. Thesis, ENSG.